

Research Article

Cite this article: Gao T *et al.* (2021) Transferrin receptor (TFRC) is essential for meiotic progression during mouse spermatogenesis. *Zygote*. 29: 169–175. doi: [10.1017/S0967199420000659](https://doi.org/10.1017/S0967199420000659)

Received: 7 May 2020

Revised: 20 October 2020

Accepted: 23 October 2020

First published online: 16 December 2020

Keywords:

DNA double-stranded break; Meiosis; Spermatocytes; Synapsis; Transferrin receptor

Authors for correspondence:

Bo Zheng, National Health and Family Planning Key Laboratory of Male Reproductive Health, Center for Reproduction and Genetics, Suzhou Municipal Hospital, The Affiliated Suzhou Hospital of Nanjing Medical University, Suzhou, China. E-mail: mansnoopy@163.com
Xiaoyan Huang, State Key Laboratory of Reproductive Medicine, Department of Histology and Embryology, Nanjing Medical University, Nanjing, China. E-mail: bbhxy@njmu.edu.cn

*These authors contributed equally to this work

Transferrin receptor (TFRC) is essential for meiotic progression during mouse spermatogenesis

Tingting Gao^{1,2,*}, Meng Lin^{2,*}, Yangyang Wu², Kai Li², Chenchen Liu², Quan Zhou², Cong Shen³, Bo Zheng³ and Xiaoyan Huang² 

¹Center of Clinical Reproductive Medicine, The Affiliated Changzhou Maternal and Child Health Care Hospital of Nanjing Medical University, Changzhou, China; ²State Key Laboratory of Reproductive Medicine, Department of Histology and Embryology, Nanjing Medical University, Nanjing, China and ³National Health and Family Planning Key Laboratory of Male Reproductive Health, Center for Reproduction and Genetics, Suzhou Municipal Hospital, The Affiliated Suzhou Hospital of Nanjing Medical University, Suzhou, China

Summary

Meiosis is a highly conserved process, and is responsible for the production of haploid gametes and generation of genetic diversity. We previously identified the transferrin receptor (TFRC) in the proteome profile of mice neonatal testes, indicating the involvement of the TFRC in meiosis. However, the exact molecular role of the TFRC in meiosis remains unclear. In this study, we aimed to determine the function of the TFRC in neonatal testicular development by TFRC knockdown using the testis culture platform. Our results showed high TFRC expression in 2-week testes, corresponding to the first meiotic division. Targeting TFRC using morpholino oligonucleotides resulted in clear spermatocyte apoptosis. In addition, we used the chromosomal spread technique to show that a deficiency of TFRC caused the accumulation of leptotene and zygotene spermatocytes, and a decrease of pachytene spermatocytes, indicating early meiotic arrest. Moreover, the chromosomes of TFRC-deficient pachytene spermatocytes displayed sustained γ H2AX association, as well as SYCP1/SYCP3 dissociation beyond the sex body. Therefore, our results demonstrated that the TFRC is essential for the progression of spermatocyte meiosis, particularly for DNA double-stranded break repair and chromosomal synapsis.

Introduction

Iron is essential for the assembly of functional Fe–S cluster proteins, heme-binding proteins, and ribonucleotide reductases (RNRs) in most eukaryotic cells. These proteins are involved in electron transfer, ribosome maturation, DNA replication and repair, and cell cycle control (Ye and Rouault, 2010; White and Dillingham, 2012; Dlouhy and Outten, 2013). Iron transport and uptake is tightly regulated in all iron-dependent organisms (Sutak *et al.*, 2008; Anderson and Vulpe, 2009; Leichtmann-Bardoogo *et al.*, 2012). Mammalian cells typically obtain most of their iron from the plasma protein transferrin (TF) (Lee *et al.*, 2003; Chua *et al.*, 2007), which binds and delivers iron to the cells. The transferrin receptor (TFRC) is expressed on the cell surface and is responsible for absorbing transferrin-bound iron through receptor-mediated endocytosis (Qian and Tang, 1995; Aisen, 2004). After iron is freed from TF, TF is returned to the cell surface for another cycle of iron transport. The entire cycle lasts a few minutes, and a distinct feature of the TF cycle is the persistence of the TF/TFRC complex (Aisen, 2004; Lamb *et al.*, 1983).

Meiosis consists of meiosis I and meiosis II, however the two processes are very different. Meiosis I includes induction of DNA double-stranded breaks (DSBs), pairing, recombination, and synapsis. Spo11 mediates the occurrence of DSBs, which elicit the DNA damage response and resulting in the activation of ATM kinase and subsequent phosphorylation of H2AX (Baudat and de Massy, 2004; Li and Ma, 2006). The loss of SPO11 function eliminates meiosis recombination and synaptic complex formation (Klapholz *et al.*, 1985; Wagstaff *et al.*, 1985). The pairing of homologous chromosomes facilitates the recombination process. DMC1 has DNA-dependent ATPase activity and forms a filamentous structure at the end of single-stranded excised DNA at the DSBs repair site, which is the key to homologous recombination repair in meiosis (Yoshida *et al.*, 1998; Pittman *et al.*, 1998). Synapses are stable connections between chromosomes made by the formation of a specific protein complex. Synchronized with the formation of the synaptic complex, the meiotic DSBs are repaired to facilitate the interaction of homologous chromosomes and finish the synapsis (Carofiglio *et al.*, 2013).

Spermatogenesis is an iron-dependent process in which iron is imported to the seminiferous tubule by transferrin, primarily secreted by Sertoli cells (Morales *et al.*, 1987; Wauben-Penris *et al.*, 1986). Leichtmann-Bardoogo and colleagues (Leichtmann-Bardoogo *et al.*, 2012) reported details of localization and regulation of many iron transport and storage proteins in the testis.

© The Author(s) 2020. This is an Open Access article, distributed under the terms of the Creative Commons Attribution licence (<http://creativecommons.org/licenses/by/4.0/>), which permits unrestricted re-use, distribution, and reproduction in any medium, provided the original work is properly cited.

Male germ cells from early developmental stages to pachytene spermatocytes express high levels of TFRC (Leichtmann-Bardoogo *et al.*, 2012). In a previous study, we constructed a proteomic profile of proteins associated with meiosis onset during mouse testis development and identified 104 differentially expressed proteins (Shao *et al.*, 2015). High levels of TFRC were observed during meiosis initiation, and was consistent with the results of Leichtmann-Bardoogo and colleagues (Leichtmann-Bardoogo *et al.*, 2012). Moreover, we found that the *Tfrc* gene is retinoic acid (RA) responsive, and that its expression was tightly regulated in RA-treated spermatogonial stem cells (Shao *et al.*, 2015). Several studies have shown the involvement of RA in triggering the onset of meiosis in male and female mammals (Kumar *et al.*, 2011; Li *et al.*, 2011), therefore TFRC is likely to play a role during mouse meiosis. In the present study, we aimed to study the role of TFRC during mouse spermatocyte meiosis using cultured mouse neonatal testes.

Materials and methods

Animals

ICR mice were maintained in a 12 h/12 h light/dark cycle at 20–22°C and 50–70% humidity with food and water available *ad libitum*. All animal treatment protocols were approved by the Ethics Committee of Nanjing Medical University (IACUC:1601181).

Neonatal testis culture

Testicular tissue from 20 mice on postnatal 5.5-day was cut into uniform pieces of 1–3 mm diameter under the microscope and placed on agarose gel half-soaked in culture medium. The day before sampling, 1.5% agarose gels (10 × 10 × 5 mm placed in six-well plates) were prepared and soaked with culture medium for more than 24 h to replace the water. Three to four agarose gels were placed inside each well of the six-well plates, and 3–5 testis tissue samples were placed on each agarose surface. Plates were maintained in a 5% carbon dioxide in air environment at 34°C. The medium was changed every 2 days. The culture system was based on previous reports (Sato *et al.*, 2011; Shen *et al.*, 2018, 2019; Zheng *et al.*, 2018; Zhao *et al.*, 2019). The medium contained α -minimum essential medium (α -MEM), 10% knockout serum replacement (KSR), 0.1% β -mercaptoethanol, 1% nonessential amino acids solution (NEAA), and 1% penicillin/streptomycin solution. Tissues were cultured for 11 days either with specific morpholinos against TFRC (Mo), or as the negative control (Ctr), at a final concentration of 10 μ mol/l. TFRC translation-blocking *vivo*-Mo (Oligo Sequence: TCTGGCTTGATCCATCA TTCTCAGC) and the control (Oligo Sequence: CCTCT TACCTCAGTTACAATTTATA) were purchased from Gene Tools LLC, Philomath, OR, USA. The experiments were designed with randomized blocks of three replicates and, in total, 12 mice were used.

Haematoxylin and eosin staining

Testis tissues were fixed in 4% paraformaldehyde for 48 h, paraffin-embedded, and sectioned into 5- μ m sections. Sections were then dewaxed in dimethylbenzene, rehydrated in graded ethanol solutions, and stained with haematoxylin and eosin (H&E). Images were captured by microscopy (Axioskop 2 plus, ZEISS).

Chromosome spread

Hypotonic extraction buffer (HEB; 30 mM Tris, 50 mM sucrose, 17 mM trisodium citrate dihydrate, 5 mM EDTA, 0.5 mM DTT, and 0.5 mM phenylmethylsulphonyl fluoride; pH 8.2), and fixative solution [1% paraformaldehyde (PFA), 0.15% Triton X-100 adjusted to pH 9.2 by using 10 mM sodium borate pH 9.2 buffer solution] were prepared. Cultured tissues were harvested, placed in Dulbecco's modified Eagle's medium for removing cells from the tubules, and subsequently put in HEB buffer for 40–60 min. Slides were covered with fixative solution. Tubules were cut to pieces at a pH of 8.2 in 100 mM sucrose, and pipetted gently to make a cell suspension, which was painted on the prepared glasses. The slides were incubated in a humidity box for at least 3 h. All samples were washed three times with phosphate-buffered saline (PBS) and air dried for subsequent immunofluorescence staining.

Immunofluorescence

Slides were prepared by chromosome spread method followed by recovery at room temperature (RT). Briefly, slides were blocked with 1% bovine serum albumin at RT for 2 h, and incubated with primary antibody at a dilution of 1:500 (Table S1) overnight at 4°C. Slides were then gently washed three times with PBS, incubated with secondary antibody at a dilution of 1:1000 at 37°C for 1 h in the dark with humidity, and washed three times with phosphate-buffered saline (PBS) and Tween. Images were captured using a Zeiss confocal microscope (lsm710, Carl Zeiss).

Western blot analysis

Cultured testis tissues were ground with a pestle in protein lysate for complete dissociation. Proteins at 40 μ g/lane were transferred to polyvinylidene difluoride membranes and incubated with primary antibodies (Table S1) at a dilution of 1:1000 overnight. Membranes were washed with Tris-buffered saline and 0.1% Tween three times, and incubated with secondary antibodies (1:5000 dilution) at RT for 2 h. Protein signals were visualized using the SuperSignal West Femto Chemiluminescent Substrate (Thermo Scientific, USA).

Terminal deoxynucleotidyl transferase dUTP nick end labelling (TUNEL) assay

Paraffin sections were dewaxed with xylene twice at RT for 10 min and then rinsed in a sequence of 100, 90, 80 and 70% alcohol at RT. After soaking in PBS, the sections were incubated with 20 μ g/ml proteinase K at RT for 20 min. After equilibrium, the sections were incubated in reaction buffer at 37– for 60 min, followed by 4',6-diamidino-2-phenylindole (DAPI) staining.

Results

In vitro culture of mouse testis

We performed *in vitro* testis culture from neonatal day 5.5 to day 16.5 and observed the morphology of cultured testes by HE staining (Fig. 1). According to the method of identifying cells in testis (Ahmed and de Rooij, 2009), only Sertoli cells and spermatogonia were observed in seminiferous tubules at day 7.5. Preleptotene spermatocytes began to appear at day 9.5. On day 12.5, we observed zygotene spermatocytes in some tubules. On day 14.5, we noticed zygotene and pachytene spermatocytes. By day 16.5, meiosis occurred in most of the seminiferous tubules.

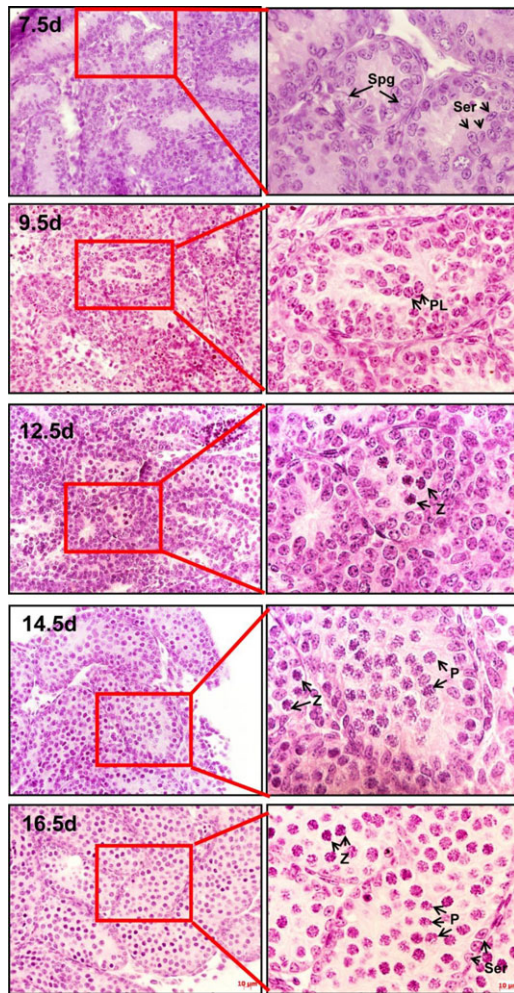


Figure 1. Haematoxylin and eosin (H&E) staining of *in vitro* mouse testicular tissue. Images show postnatal 5.5 d testicular tissues cultured for 2 days (7.5 d), 4 days (9.5 d), 7 days (12.5 d), 9 days (14.5 d), and 11 days (16.5 d), respectively. At day 7.5, the seminiferous tubule contained spermatogonial stem cells and Sertoli cells. The preleptotene spermatocytes began to appear at day 9.5. At day 12.5, zygotene spermatocytes emerged in some seminiferous tubules. In addition to zygotene spermatocytes, pachytene spermatocytes also appeared at day 14.5. By day 16.5, meiosis occurred in most of the seminiferous tubules. Scale bar, 10 μ m. P, pachytene spermatocytes; PL, preleptotene spermatocytes; Ser, Sertoli cells; Spg, spermatogonial stem cells; Z, zygotene spermatocytes.

TFRC is essential for spermatocyte survival in mice

In our previous study, we found that TFRC protein expression was higher in 10.5-day testis than in 8.5-day testis (Shao *et al.*, 2015), which spans meiosis onset in mouse. Moreover, Leichtmann-Bardoogo and colleagues (Leichtmann-Bardoogo *et al.*, 2012) reported that TFRC was located on leptotene and zygotene spermatocytes in adult mouse testis. In this study, western blot analysis showed that TFRC expression increased between weeks 1 and 2 and decreased between weeks 2 and 3 (Fig. 2A, B). These results indicated that TFRC may play a pivotal role in early meiosis. To elucidate the function of TFRC in meiosis, we knocked down TFRC protein expression using morpholinos specific for TFRC in neonatal testis. Western blot analysis showed a knockdown efficiency of 70% (Fig. 2C, D). HE staining showed zygotene and pachytene spermatocytes in the negative control group. The

morpholino-treatment group (Mo) only had zygotene spermatocytes, which were apoptotic (Fig. 2E). The apoptotic signals were further verified by co-staining of SYCP3 with TUNEL (Fig. 2F, G) and cleaved caspase-3 (Fig. 2H, I), respectively. The results revealed a significant increase of apoptosis of spermatocytes in the Mo group. In addition, we also stained somatic cell markers to determine if TFRC knockdown affected somatic cells. We found that there were no differences in somatic cells and no changes in basal membrane of tubules in Mo compared with the control group (Ctr) (Fig. S1).

TFRC promotes synaptonemal complex (SC) formation

In order to determine the exact stage of meiotic arrest in Mo testes, we used the chromosomal spread technique. This technique allowed us to observe accurately the chromosomal status of spermatocytes at the single-cell level and therefore determine the stage. We assessed chromosomal synapsis by co-staining SYCP1 (a central element protein of SC) and SYCP3 (a lateral element protein of SC) (Cohen *et al.*, 2006). SC lateral elements are formed as early as the leptotene stage, initiate synapsis through physical juxtaposition at the zygotene stage, and promote complete synapsis on autosomes at the pachytene stage (Kumar *et al.*, 2011). The Ctr group showed complete alignment of SYCP3 and SYCP1 at the pachytene stage, except at apparent sex bodies in which unpaired XY chromosomes lacked the central element. Spermatocytes from Mo remained in a pachytene-like stage, characterized by obvious chromosome pairing and formation of SC lateral elements (SYCP3), but loss of SYCP1 staining at most chromosome sites, demonstrating the existence of aberrant synapsis in the autosomes (Fig. 3).

Failure of DNA double-stranded break repair in TFRC-deficient spermatocytes

To investigate DNA repair after TFRC knockdown, we used γ H2AX, a marker for DSBs, for fluorescence detection. Spermatocytes of the Ctr group included leptotene, zygotene, and pachytene spermatocytes. At the leptotene and zygotene stages, γ H2AX was present on autosomal chromatin and was distributed widely throughout the nucleus. At the pachytene stage, it disappeared from the autosomes following meiotic DSB repair and was limited to the XY body. The expression of γ H2AX signals revealed that DSBs were formed in Mo leptotene and zygotene stages. However, the pachytene-like spermatocytes in Mo exhibited diffuse localization of γ H2AX throughout the nucleus and failed to form XY bodies (Fig. 4A), demonstrating an aberrant repair of meiotic DSBs in Mo. To further confirm the stage of arrest in TFRC-deficient spermatocytes, we performed quantification analysis. Approximately 273 and 268 spermatocytes were included in the Ctr and Mo spermatocyte preparations respectively. Ctr spermatocytes showed the largest proportion of pachytene cells (58.24%), followed by zygotene (37.36%), and leptotene (4.40%). TFRC-deficient spermatocytes displayed a marked redistribution, with zygotene cells being the most abundant (63.05%), followed by pachytene-like (27.98%), and leptotene (8.97%) (Fig. 4B). The accumulation of zygotene spermatocytes in the Mo group corroborated the results of SYCP1 and SYCP3 (Fig. 3), and SYCP3 and γ H2AX (Fig. 4A) co-staining.

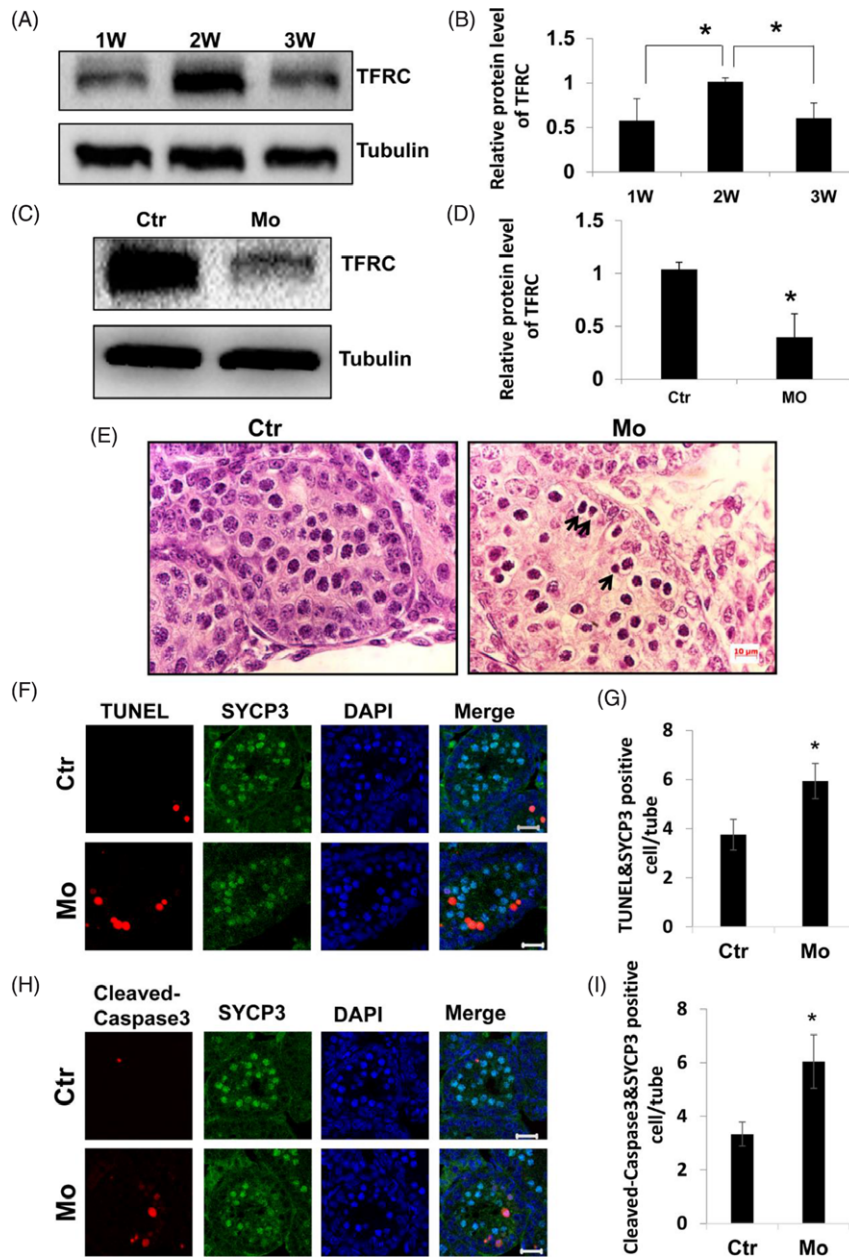


Figure 2. TFRC and spermatocyte survival. (A) Western blot results showing that TFRC protein expression increased significantly between weeks 1 and 2 and decreased significantly between weeks 2 and 3. (B) Gray value analysis data of western blot. $*P < 0.05$, one-way analysis of variance (ANOVA), $n = 3$. (C) Western blot results showing that TFRC protein content significantly decreased after 10 μ M morpholino (Mo) treatment compared with the control group (Ctr). (D) Gray value data analysis showing that TFRC knockdown efficiency was 70% after Mo treatment, and the difference was statistically significant ($P = 0.05$). Student's *t*-test, $n = 3$. (E) H&E staining of mouse testicular tissue treated with 10 μ M morpholino for 11 days. Normal spermatocytes in the zygotene and pachytene stages were observed in the Ctr group, while only apoptotic spermatocytes were observed in the MO group (black arrow). Scale bar, 10 μ m. (F) Co-staining of TUNEL (red) and SYCP3 (green) in Ctr and Mo testes. Scale bars, 20 μ m. (G) Quantification of (F). $*P < 0.05$, Student's *t*-test, $n = 3$. (H) Co-immunostaining of cleaved caspase 3 (red) and SYCP3 (green) in Ctr and Mo testes. Scale bars, 20 μ m. (I) Quantification of (H). $*P < 0.05$, Student's *t*-test, $n = 3$. Ctr, negative control; DAPI, 4',6'-diamidino-2-phenylindole; Mo, morpholino treatment; SYCP3, synaptonemal complex protein 3; TUNEL, terminal deoxyribonucleotidyl transferase (TDT)-mediated dUTP-digoxigenin nick-end labelling.

Discussion

We used cultured neonatal mouse testes to determine the function of TFRC in neonatal testes, and found that knockdown of TFRC in neonatal testicular culture caused spermatocyte apoptosis. In addition, we observed that disruption of TFRC led to aberrant synapsis and failure of DSB repair. An accumulation of zygotene spermatocytes was also observed after TFRC disruption. Our results demonstrated that TFRC is essential for male meiosis, and defects in

TFRC-deficient testes become most evident at the transition from the zygotene to pachytene stage.

Iron is essential for the activation of Src kinase, which rapidly phosphorylates and reduces p27, thereby stimulating cyclin-dependent kinase 2 (CDK2 kinase) activity (Hengst and Reed, 1996; Bloom and Pagano, 2003). CDK2 is necessary for chromosome synapsis, and CDK2 knockout mice exhibited abnormal meiosis and extensive spermatocyte apoptosis (Ortega *et al.*,

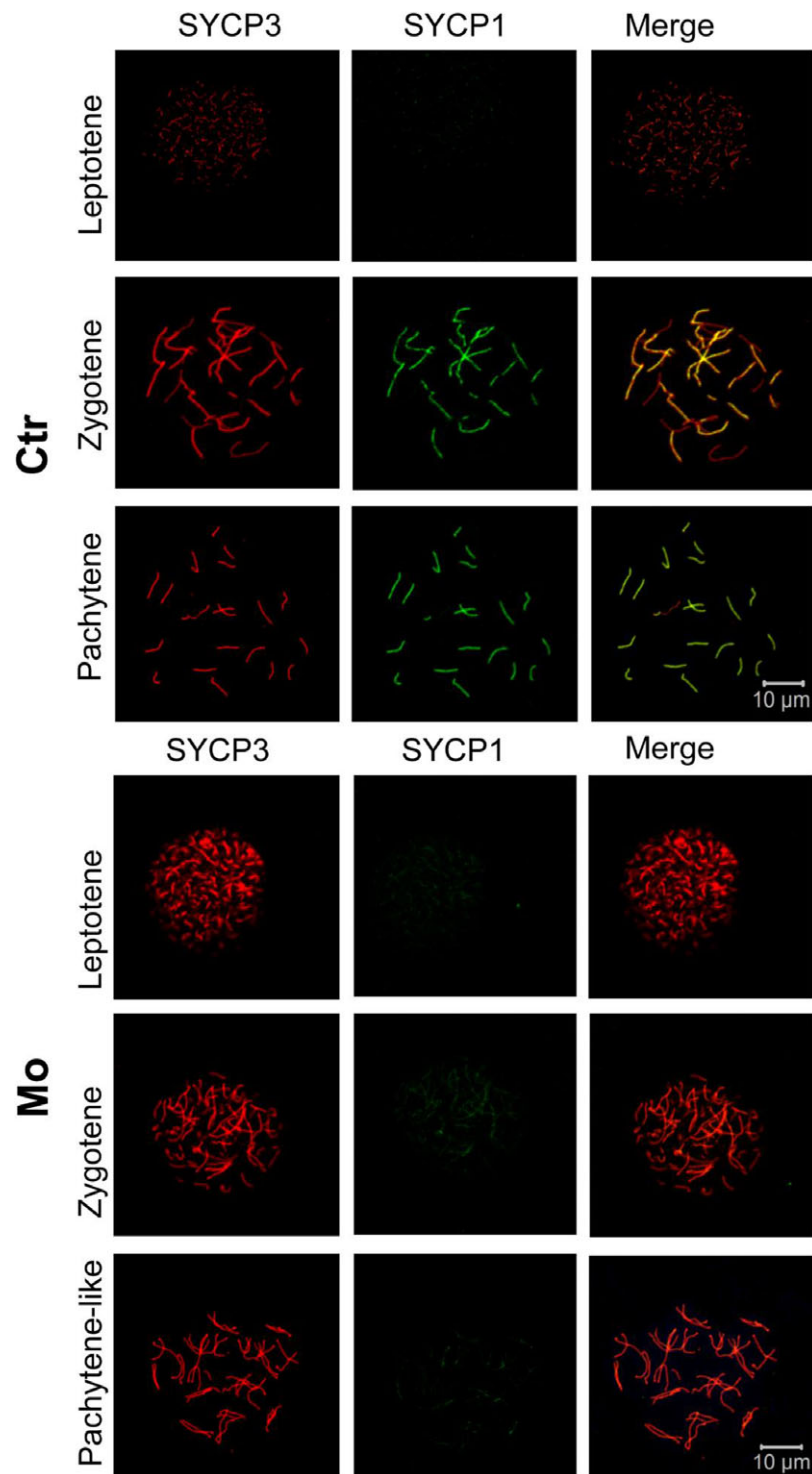


Figure 3. Chromosome spread of spermatocytes detected by co-immunostaining of SYCP3 (red) with SYCP1 (green). TFRC-Ctr, negative control group, TFRC-morpholino, 10 $\mu\text{mol/l}$ morpholino-treated group. Scale bars, 10 μm . Ctr, negative control; Mo, morpholino treatment; SYCP1, synaptonemal complex protein 1; SYCP3, synaptonemal complex protein 3.

2003). In the absence of CDK2, SC proteins failed to assemble on homologous chromosomes. In this study, we found aberrant distribution of SC in TFRC-deficient spermatocytes. We therefore speculated that knockdown of TFRC in spermatocytes led to decreased intracellular iron and CDK2 activity, and finally caused aberrant synapsis in the autosomes. Alternatively, iron could act as

a constraining factor in meiosis (Brault *et al.*, 2016). DNA helicases, such as FancJ, ChlR1, and Dna2, contain a conserved cluster of Fe-S at the N-terminal, which is necessary for DNA helicase activity during DSB (Wu and Brosh, 2012). The DSB formed during recombination can induce phosphorylation of H₂AX. In our study, we detected abnormal repair of DSBs in the MO group,

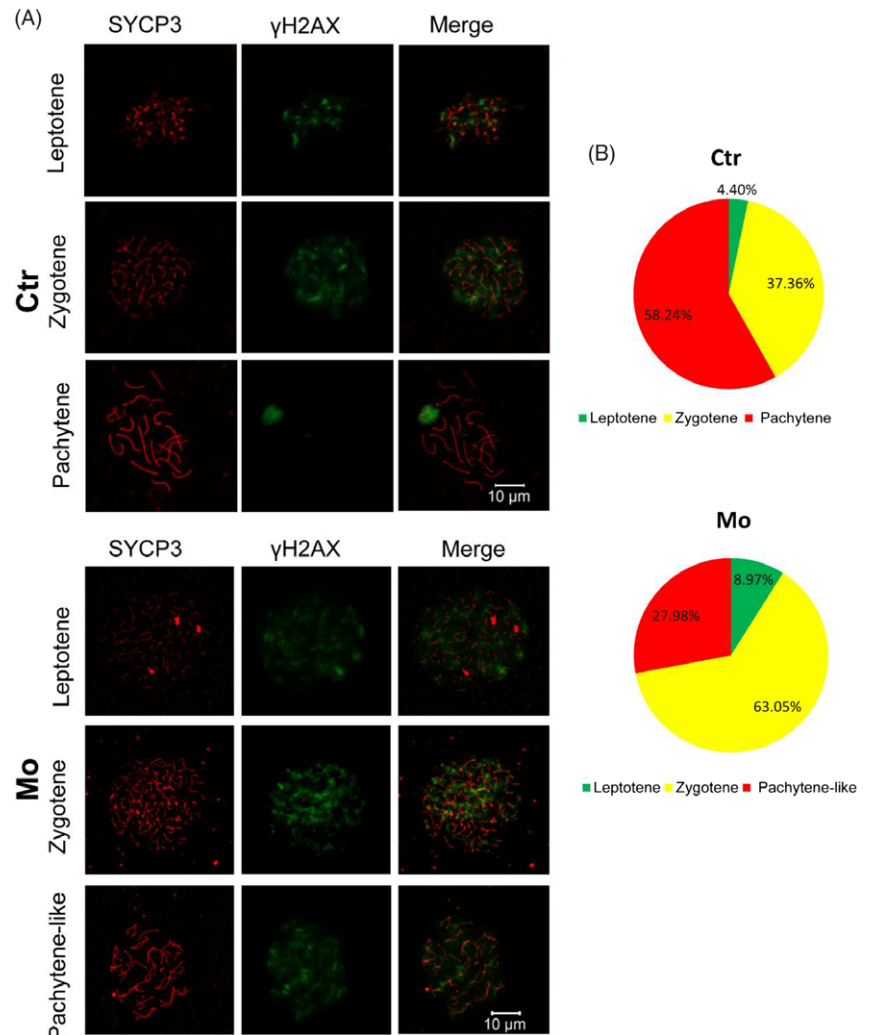


Figure 4. Chromosome spread of spermatocytes detected by co-immunostaining of SYCP3 (red) with γ H2AX (green). (A) SYCP3 was shallowly scattered at the leptotene phase, prolonged, and deepened at the zygotene phase, and its staining appeared as thick and short lines at the pachytene stage. Pachytene-like spermatocytes appeared in the TFRC-morpholino-treatment group. In the normal pachytene phase, γ H2AX was located on the sex chromosome; in pachytene-like spermatocytes, γ H2AX showed dispersive distribution. Scale bars, 10 μ m. (B) Distribution of stage-specific primary spermatocyte populations in Ctr and Mo testes. Ctr, negative control; γ H2AX, gamma H2A.X variant histone; Mo, morpholino treatment; SYCP3, synaptonemal complex protein 3.

which γ H₂AX was diffused rather than confinement to the sex chromosomes in the pachytene phase. We therefore obtained that TFRC-mediated iron transport contributed to DSB repair.

In conclusion, in this study, we determined the function of TFRC in mammalian testes by using cultured neonatal testes. Our results demonstrated that TFRC is essential for homologous chromosome synapsis and DSB repair during meiosis.

Supplementary material. To view supplementary material for this article, please visit <https://doi.org/10.1017/S0967199420000659>

Financial support. This work was supported by National Natural Science Foundation of China (81901532 and 81901533), Natural Science Foundation of Jiangsu Province (BK20190188), Science and Technology Project of Changzhou (CJ20180040), Clinical Medical Foundation of Chinese Medical Association (18010330762), Suzhou Introduced Project of Clinical Medical Expert Team (SZYJTD201708), Suzhou Key Laboratory of Male Reproduction Research (SZS201718), Open Fund of State Key Laboratory of Reproductive Medicine of Nanjing Medical University (SKLRM-KA201704) and Open Fund of National Health and Family Planning Key Laboratory of Male Reproductive Health (2019GJP03-1).

Conflicts of interest. None.

Ethical standards. All mouse care and use protocols were employed in accordance with the guidelines of the Ethics Committee of Nanjing Medical University, China.

References

- Ahmed EA and de Rooij DG (2009). Staging of mouse seminiferous tubule cross-sections. *Methods Mol Biol* **558**, 263–77.
- Aisen P (2004). Transferrin receptor 1. *Int J Biochem Cell Biol* **36**, 2137–43.
- Anderson GJ and Vulpe CD (2009). Mammalian iron transport. *Cell Mol Life Sci* **66**, 3241–61.
- Baudat F and de Massy B (2004). [SPO11: an activity that promotes DNA breaks required for meiosis]. *Med Sci (Paris)* **20**, 213–8.
- Bloom J and Pagano M (2003). Deregulated degradation of the cdk inhibitor p27 and malignant transformation. *Semin Cancer Biol* **13**, 41–7.
- Brault A, Rallis C, Normant V, Garant JM, Bahler J and Labbe S (2016). Pph4 is a key player for iron economy in meiotic and sporulating cells. *G3 (Bethesda)* **6**, 3077–95.
- Carofiglio F, Inagaki A, de Vries S, Wassenaar E, Schoenmakers S, Vermeulen C, van Cappellen WA, Sleddens-Linkels E, Grootegoed JA, Te Riele HP, de Massy B and Baarends WM (2013). SPO11-independent DNA repair foci and their role in meiotic silencing. *PLoS Genet* **9**, e1003538.

- Chua AC, Graham RM, Trinder D and Olynyk JK (2007). The regulation of cellular iron metabolism. *Crit Rev Clin Lab Sci* **44**, 413–59.
- Cohen PE, Pollack SE and Pollard JW (2006). Genetic analysis of chromosome pairing, recombination, and cell cycle control during first meiotic prophase in mammals. *Endocr Rev* **27**, 398–426.
- Dlouhy AC and Outten CE (2013). The iron metallome in eukaryotic organisms. *Met Ions Life Sci* **12**, 241–78.
- Hengst L and Reed SI (1996). Translational control of p27Kip1 accumulation during the cell cycle. *Science* **271**, 1861–4.
- Klapholz S, Waddell CS and Esposito RE (1985). The role of the *SPO11* gene in meiotic recombination in yeast. *Genetics* **110**, 187–216.
- Kumar S, Chatzi C, Brade T, Cunningham TJ, Zhao X and Duester G (2011). Sex-specific timing of meiotic initiation is regulated by *Cyp26b1* independent of retinoic acid signalling. *Nat Commun* **2**, 151.
- Lamb JE, Ray F, Ward JH, Kushner JP and Kaplan J (1983). Internalization and subcellular localization of transferrin and transferrin receptors in HeLa cells. *J Biol Chem* **258**, 8751–8.
- Lee AW, Oates PS and Trinder D (2003). Effects of cell proliferation on the uptake of transferrin-bound iron by human hepatoma cells. *Hepatology* **38**, 967–77.
- Leichtmann-Bardoogo Y, Cohen LA, Weiss A, Marohn B, Schubert S, Meinhardt A and Meyron-Holtz EG (2012). Compartmentalization and regulation of iron metabolism proteins protect male germ cells from iron overload. *Am J Physiol Endocrinol Metab* **302**, E1519–30.
- Li H, Palczewski K, Baehr W and Clagett-Dame M (2011). Vitamin A deficiency results in meiotic failure and accumulation of undifferentiated spermatogonia in prepubertal mouse testis. *Biol Reprod* **84**, 336–41.
- Li W and Ma H (2006). Double-stranded DNA breaks and gene functions in recombination and meiosis. *Cell Res* **16**, 402–12.
- Morales C, Sylvester SR and Griswold MD (1987). Transport of iron and transferrin synthesis by the seminiferous epithelium of the rat *in vivo*. *Biol Reprod* **37**, 995–1005.
- Ortega S, Prieto I, Odajima J, Martin A, Dubus P, Sotillo R, Barbero JL, Malumbres M and Barbacid M (2003). Cyclin-dependent kinase 2 is essential for meiosis but not for mitotic cell division in mice. *Nat Genet* **35**, 25–31.
- Pittman DL, Cobb J, Schimenti KJ, Wilson LA, Cooper DM, Brignull E, Handel MA and Schimenti JC (1998). Meiotic prophase arrest with failure of chromosome synapsis in mice deficient for *Dmc1*, a germline-specific *RecA* homolog. *Mol Cell* **1**, 697–705.
- Qian ZM and Tang PL (1995). Mechanisms of iron uptake by mammalian cells. *Biochim Biophys Acta* **1269**, 205–14.
- Sato T, Katagiri K, Gohbara A, Inoue K, Ogonuki N, Ogura A, Kubota Y and Ogawa T (2011). *In vitro* production of functional sperm in cultured neonatal mouse testes. *Nature*, **471**, 504–7.
- Shao B, Guo Y, Wang L, Zhou Q, Gao T, Zheng B, Zheng H, Zhou T, Zhou Z, Guo X, Huang X and Sha J (2015). Unraveling the proteomic profile of mice testis during the initiation of meiosis. *J Proteomics* **120**, 35–43.
- Shen C, Yu J, Zhang X, Liu CC, Guo YS, Zhu JW, Zhang K, Yu Y, Gao TT, Yang SM, Li H, Zheng B and Huang XY (2019). Strawberry Notch 1 (*SBNO1*) promotes proliferation of spermatogonial stem cells via the non-canonical Wnt pathway in mice. *Asian J Androl* **21**, 345–50.
- Shen C, Zhang K, Yu J, Guo Y, Gao T, Liu Y, Zhang X, Chen X, Yu Y, Cheng H, Zheng A, Li H, Huang X, Ding X and Zheng B (2018). Stromal interaction molecule 1 is required for neonatal testicular development in mice. *Biochem Biophys Res Commun* **504**, 909–15.
- Sutak R, Lesuisse E, Tachezy J and Richardson DR (2008). Crusade for iron: iron uptake in unicellular eukaryotes and its significance for virulence. *Trends Microbiol*, **16**, 261–8.
- Wagstaff JE, Klapholz S, Waddell CS, Jensen L and Esposito RE (1985). Meiotic exchange within and between chromosomes requires a common *Rec* function in *Saccharomyces cerevisiae*. *Mol Cell Biol* **5**, 3532–44.
- Wauben-Penris PJ, Strous GJ and Van der Donk HA (1986). Transferrin receptors of isolated rat seminiferous tubules bind both rat and human transferrin. *Biol Reprod* **35**, 1227–34.
- White MF and Dillingham MS (2012). Iron-sulphur clusters in nucleic acid processing enzymes. *Curr Opin Struct Biol* **22**, 94–100.
- Wu Y and Brosh RM, Jr (2012). DNA helicase and helicase-nuclease enzymes with a conserved iron-sulfur cluster. *Nucleic Acids Res* **40**, 4247–60.
- Ye H and Rouault TA (2010). Human iron-sulfur cluster assembly, cellular iron homeostasis, and disease. *Biochemistry* **49**, 4945–56.
- Yoshida K, Kondoh G, Matsuda Y, Habu T, Nishimune Y and Morita T (1998). The mouse *RecA*-like gene *Dmc1* is required for homologous chromosome synapsis during meiosis. *Mol Cell* **1**, 707–18.
- Zhao D, Shen C, Gao T, Li H, Guo Y, Li F, Liu C, Liu Y, Chen X, Zhang X, Wu Y, Yu Y, Lin M, Yuan Y, Huang X, Yang S, Yu J, Zhang J and Zheng B (2019). Myotubularin related protein 7 is essential for the spermatogonial stem cell homeostasis via PI3K/AKT signaling. *Cell Cycle* **18**, 2800–13.
- Zheng B, Yu J, Guo Y, Gao T, Shen C, Zhang X, Li H and Huang X (2018). Cellular nucleic acid-binding protein is vital to testis development and spermatogenesis in mice. *Reproduction* **156**, 59–69.